Thiyl Radical Interaction with Pyrimidine C5−C6 Double Bond

Aleksandra Wójcik, Sergej Naumov,† Bronisław Marciniak,‡ Ralf Hermann, and Ortwin Brede*

University of Leipzig, Interdisciplinary Group for Time-Resolved Spectroscopy, Permoserstr. 15, 04303 Leipzig, Germany, Institute of Surface Modification, 04303 Leipzig, Germany, and Institute of Chemical Physics, Facility of Chemistry, Adam Mickiewicz University, Grunwaldzka 6, 60−780 Poznań, Poland

Received: April 4, 2005; In Final Form: May 31, 2005

Addition and elimination interaction of thiyl radicals with the C5−C6 double bond in pyrimidines was studied by the pulse radiolysis technique in aqueous solution with the use of different monitoring systems. For this purpose, *p*-thiocresol, cysteamine hydrochloride, and mercaptoethanol were used. The rate constants of addition and elimination of thiyl radicals were determined by applying the modified version of ACUCHEM (computer program for modeling complex reaction systems). Aliphatic thiyl radicals add to the pyrimidine C5−C6 double bond with $k = 1.0-3.0 \times 10^7$ dm^3 mol^{-1} s^{-1}, whereas elimination takes place with $k = 0.7-2.0 \times 10^5$ s^{-1}. Quantum chemical calculations at the B3LYP/6-31G(d)/PCM level show that the addition should occur at the C6 position of the pyrimidine ring and that the energy of interaction between thiyl radicals and the pyrimidine double bond C5−C6 is low.

1. Introduction

Thiols (RSH) play a very important role in the living cells serving as antioxidants and, therefore, "protecting" against ionizing radiation. They can be hydrogen donors in radical repair reactions, preventing, for example, the strand breakage in DNA by reacting with the base or sugar radical.[1]

$$DNA^{\bullet} + RSH \rightarrow DNA + RS^{\bullet} \quad (1)$$

However, they are also likely to protect DNA by electron transfer from thiol or thiolate (RS^-) to DNA radical cations ($DNA^{\bullet+}$).[2]

$$DNA^{\bullet+} + RSH \rightarrow DNA + RS^{\bullet} + H^+ \quad (2)$$

$$DNA^{\bullet+} + RS^- \rightarrow DNA + RS^{\bullet} \quad (3)$$

All those reactions prevent radical damages in biologically important molecules, not only in DNA, but also in lipids or proteins.[3−5] However, simultaneously, thiyl radicals ($RS^{\bullet}$) are formed. The reactivity of those radicals is much lower than that of C-centered radicals; nevertheless, it is high enough to cause changes in biologically important molecules. It is known that thiyl radicals are capable of abstracting hydrogen from carbon−hydrogen bonds (C−H) in alcohols and ethers,[6] from the methyl group in thymine,[7] from α-carbon−hydrogen bonds ($^{\alpha}$C−H) in peptides,[8,9] and from bisallylic methylene groups in polyunsaturated fatty acids (PUFA).[10] Moreover, they can reversibly add to unsaturated bonds. It is reported that, in the course of the addition−elimination interaction of thiyl radicals with double bonds in PUFA, cis−trans isomerization takes place.[11,12] The problem of the interaction of thiyl radicals with the double bonds in PUFA and its possible biological consequences are now under detailed investigation.[13−16] However, only a little is known about the interaction between thiyl radicals and the double bond C5−C6 in pyrimidines (Pyr).

$$Pyr + RS^{\bullet} \rightleftarrows Pyr^{\bullet}(RS) \quad (4)$$

According to the monograph of von Sonntag,[5] this kind of addition−elimination reaction should possibly exist, similarly to the addition−elimination reaction of thiyl radicals to simple olefins. However, the equilibria of the reaction may be strongly shifted to the left-hand side. Until now, no adduct or any of its derivatives have been detected, and hence, there is no information on the rate constants of forward and backward reactions. There is, however, chemical evidence of thiyl radical addition to the C6 position of the pyrimidine ring on the basis of steady-state product analysis. The phenyl-cyclopropyl substituent at the C5 position was used to leave the "fingerprint" of the initial place of thiyl radical addition.[17] In the detected products, a cyclopropane ring was cleaved, which was a sign of thiyl radical addition to the C6 position.

Therefore, the question should be posed whether thiyl radicals add to the pyrimidine C5−C6 double bond and what the kinetic parameters of that process are. In this paper, we report our results concerning thiyl radicals interaction with the C5−C6 double bond in pyrimidines, investigated by pulse radiolysis in aqueous solution with the use of different monitoring systems. On this basis, we determined the addition and elimination rate constants (k_4 and k_{-4}) by applying a computer program for kinetic simulations (modified version of ACUCHEM[18]). We also carried out quantum chemical calculations in order to explain the nature of the discussed interaction.

2. Materials and Methods

2.1. Chemicals. The thiols were purchased from Merck (2-mercaptoethanol, MerSH), from Sigma (cysteamine hydrochloride, CystSH), and from Aldrich (*p*-thiocresol, *p*-ArSH and

* Corresponding author. E-mail address: brede@mpgag.uni-leipzig.de.
† Institute of Surface Modification.
‡ Institute of Chemical Physics.

10.1021/jp051711s CCC: $30.25
Published on Web 07/16/2005

CHART 1: Structures of the Aliphatic Thiols (1) Cysteamine, (2) 2-mercaptoethanol, (3) Penicillamine and Pyrimidines, (4) Thymine, (5) Uracil, and (6) Cytosine Used in the Experiments

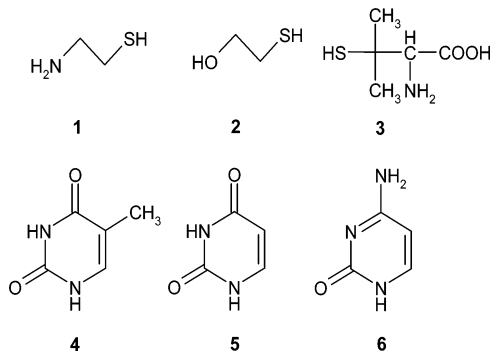

penicillamine, PenSH); they had a purity of 98−99%. Linoleic acid (*cis*,*cis*-9,12-octadecadienoic acid, LA) of 99% purity, 2-chloroethanol (ClEtOH), and pyrimidines (thymine, uracil, cytosine; purity 97−98%) were obtained from Aldrich. Structures of the pyrimidines and thiols used in the experiments are presented in Chart 1. Borate buffer used in the experiments (2.5×10^{-2} mol dm^{-3}) was prepared from sodium tetraborate decahydrate (analytical grade) also purchased from Aldrich. 2-Propanol (^{i}PrOH), ethanol (EtOH), and acetone with 99.9% purity were from Merck. Water used in all the experiments was treated with the Millipore Milli-Q Plus system.

2.2. Pulse Radiolysis. Pulse radiolysis experiments were carried out using a pulse-transformer-type accelerator ELIT (Institute of Nuclear Physics, Novosibirsk, Russia), generating 15 ns pulses of 1 MeV electrons with a 10−20 Gy dose.[19] The absorbed dose per pulse was measured with the electron dosimeter (absorption of hydrated electron at 580 nm in slightly alkaline solution). Transient species were detected with the optical absorption set up consisting of a pulsed xenon lamp (XPO 900, Osram), a Spectra Pro-500 monochromator (Acton Research Corporation), an IP28 photomultiplier (Hamamatsu Photonics), and a 1 GHz digitizing oscilloscope (TDS 640, Tektronix). All experiments were performed at room temperature in water/ethanol (1:1, v/v) or water/2-propanol (17:3, 31:19, v/v) mixtures. Only freshly prepared solutions were used; during irradiation, they were flowing continuously through a quartz cell with 1 cm optical path length. Twenty min prior to the irradiation, and also during the measurement, solutions were bubbled with highest purity N_2O (for *p*-thiocresol and disulfide radical anion containing systems) and N_2 (for linoleic acid solutions). The assumed concentration of residual oxygen was $\leq 1 \times 10^{-5}$ mol dm^{-3}. Such an equilibrium concentration was expected because of the use of polyethylene tubes in the flowing system. pH of the solutions was measured with a 540GLP pH meter (WTW).

3. Results

3.1. Pulse Radiolysis Experiments. *3.1.1. Monitoring Based on the Aromatic Thiyl Radical Absorption.* Aromatic thiyl radicals show pronounced optical absorption in the range of $\lambda = 450-500$ nm.[20] Our assumption was that the addition of the pyrimidine should accelerate the decay of the observed *p*-thiocresol thiyl radicals (*p*-ArS$^\bullet$) as the result of their pseudo-first-order reaction with the pyrimidine C5−C6 double bond. Solutions containing 5×10^{-3} mol dm^{-3} *p*-thiocresol in mixture water/2-propanol (31:19, v/v) were irradiated under N_2O with doses 10 and 20 Gy. The obtained spectrum of aromatic thiyl

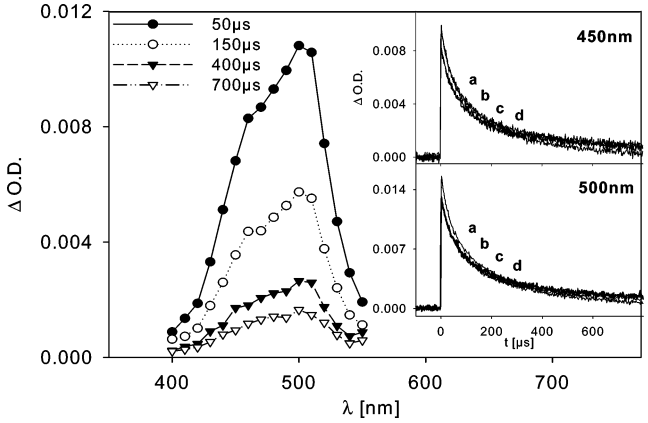

Figure 1. Decay in time of *p*-thiocresol thiyl radical absorption; N_2O saturated water/2-propanol (31:19, v/v) solution of *p*-thiocresol (5×10^{-3} mol dm^{-3}); dose/pulse, 10 Gy. The insets show time profiles at 450 and 500 nm taken with various thymine concentrations: (a) 0, (b) 5×10^{-3}, (c) 1×10^{-2}, and (d) 2×10^{-2} mol dm^{-3}.

radicals is given in Figure 1. They were formed in the following reaction sequence:

$$H_2O \rightsquigarrow H^\bullet, HO^\bullet, e_{aq}^- \quad (5)$$

$$N_2O + e_{aq}^- + H_2O \rightarrow N_2 + OH^- + HO^\bullet \qquad k_6 = 9.0 \times 10^9 \text{ dm}^3 \text{ mol}^{-1} \text{ s}^{-1} \quad (6)$$

$$^i\text{PrOH} + H^\bullet \rightarrow {}^i\text{Pr}^\bullet\text{OH} + H_2 \qquad k_7 = 7.4 \times 10^7 \text{ dm}^3 \text{ mol}^{-1} \text{ s}^{-1} \quad (7)$$

$$^i\text{PrOH} + HO^\bullet \rightarrow {}^i\text{Pr}^\bullet\text{OH} + H_2O \qquad k_8 = 2.2 \times 10^9 \text{ dm}^3 \text{ mol}^{-1} \text{ s}^{-1} \quad (8)$$

$$^i\text{Pr}^\bullet\text{OH} + p\text{-ArSH} \rightarrow {}^i\text{PrOH} + p\text{-ArS}^\bullet \quad (9)$$

The rate constants given next to the reaction equations are the values used in the computer simulations for the disulfide radical anion and pentadienyl radical detection systems (Part 3.2). As it will be elucidated further on, given values are always based on the literature data or on our own experiments.

In the radiolysis of water H$^\bullet$, HO$^\bullet$ and e_{aq}^- are formed as primary species. Hydrated electrons are scavenged by the reaction with N_2O. HO$^\bullet$ and H$^\bullet$ radicals react with 2-propanol, abstracting hydrogen. As a result, α-hydroxyalkyl radicals are formed. They abstract hydrogen from thiol, which leads to thiyl radical formation. When a pyrimidine is added to the system, *p*-ArS$^\bullet$ radicals are expected to react with its C5−C6 double bond in reaction 10:

$$p\text{-ArS}^\bullet + \text{Pyr} \rightleftarrows \text{Pyr}^\bullet(p\text{-ArS}) \quad (10)$$

However, neither adding thymine (inset, Figure 1) nor uracil in concentrations up to 2×10^{-2} mol dm^{-3} was influencing the decays at 450 and 500 nm; there were also no changes at other wavelengths in the range of 400−550 nm. To ensure that lack of the expected effect is not caused by the back reaction (−10), as it was earlier reported for aromatic thiyl radical addition to simple olefins,[21−23] all experiments were carried out under oxygen to shift the equilibrium into the direction of adduct formation. Possible adduct Pyr$^\bullet$(*p*-ArS), being a C-centered radical, should react rapidly with oxygen (estimated value: $k_{12} = 1 \times 10^9$ dm^3 mol^{-1} s^{-1}), whereas aromatic thiyl

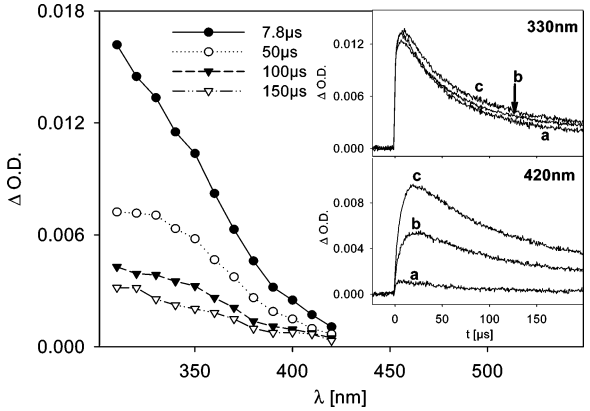

Figure 2. Decay in time of penicillamine thiyl radical absorption; N_2 saturated solution of 1×10^{-3} mol dm^{-3} penicillamine and 1 mol dm^{-3} acetone in water/2-propanol (17:3, v/v) mixture; pH = 2.5, adjusted with HCl; 100 Gy/pulse. Insets show time profiles at 330 nm and 420 nm after adding uracil: (a) 0, (b) 1×10^{-2}, and (c) 2×10^{-2} mol dm^{-3} uracil.

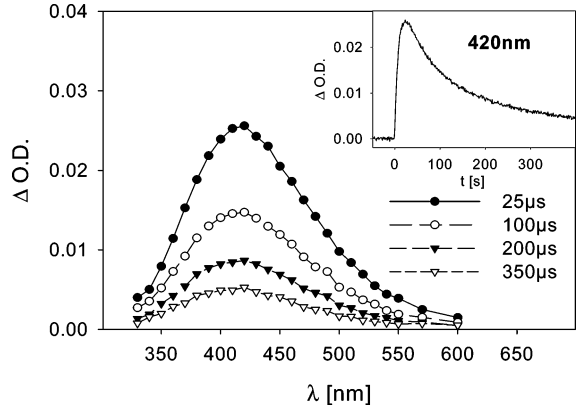

Figure 3. Decay in time of disulfide radical anion absorption; N_2O saturated water/2-propanol (17:3, v/v) solution of cysteamine hydrochloride (2×10^{-3} mol dm^{-3}); pH = 9.7, adjusted with borate buffer; dose/pulse, 20 Gy. The inset shows time profile at 420 nm.

radical should react much slower ($k_{11} < 9 \times 10^4$ dm^3 mol^{-1} s^{-1}):[21−23]

$$p\text{-ArS}^\bullet + O_2 \rightarrow p\text{-ArSOO}^\bullet \quad (11)$$

$$\text{Pyr}^\bullet(p\text{-ArS}) + O_2 \rightarrow \text{peroxyl radicals} \quad (12)$$

Also, after modifying the experimental conditions, addition of thymine (up to 4×10^{-2} mol dm^{-3}) did not affect the observed effects. Hence, the rate constant of reaction 10 should be $k_{10} \leq 1 \times 10^4$ dm^3 mol^{-1} s^{-1}. This is out of our experimental observation range.

3.1.2. Monitoring Based on the Disulfide Radical Anion Absorption. In contrast to the aromatic thiyl radicals, the aliphatic ones do not exhibit pronounced optical absorption.[24,25] Therefore, it is difficult to observe them. Penicillamine thiyl radical is an exception. It has $\epsilon_{330} = 1220$ dm^3 mol^{-1} cm^{-1}.[25] Solutions containing 1×10^{-3} and 2×10^{-3} mol dm^{-3} penicillamine in water/2-propanol mixture (17:3, v/v) were irradiated in the presence of 1 mol dm^{-3} acetone as an electron scavenger (reaction 13) under N_2 with the dose of 100 Gy per pulse. Experiments were carried out at pH = 2.5 (adjusted with HCl) to avoid thiolate formation and significant disulfide radical anion formation. At this pH, the isopropyl radical anion formed in reaction 13 ($k_{13} = 6.5 \times 10^9$ dm^3 mol^{-1} s^{-1})[26] got immediately protonated (reaction 14) because the pK_a of the isopropyl radical is 12.03.[5]

$$e_{aq}^- + (CH_3)_2CO \rightarrow (CH_3)_2CO^{\bullet -} \quad (13)$$

$$(CH_3)_2CO^{\bullet -} + H^+ \rightarrow (CH_3)_2C^\bullet OH \quad (14)$$

Addition of pyrimidines (up to 2×10^{-2} mol dm^{-3}) did not cause any changes at 330 nm, but we registered additional optical absorption around 400, 420, and 480 nm using thymine, uracil, and cytosine, respectively (Figure 2). However, as it will be explained in the discussion part, the observed additional absorption was caused by a side reaction. The addition of thiyl radicals to the C5−C6 pyrimidine double bond was invisible.

At higher pH, thiyl radicals react with thiolate (reaction 16, see Table 1), forming the disulfide radical anion ($RSSR^{\bullet -}$) that exhibits pronounced optical absorption around 420 nm.[27] We assumed that, after adding pyrimidine to the system, one would observe changes in the absorption of the species at 420 nm as the result of competition between reaction of disulfide radical anion formation and addition of thiyl radicals to the C5−C6 double bond in pyrimidines (reactions 16 and 4, respectively).

Measurements were performed for two aliphatic thiols: cysteamine (in the form of a hydrochloride salt) and 2-mercaptoethanol. For this purpose, thiols (2×10^{-3} mol dm^{-3}) were dissolved in water/2-propanol (17:3, v/v) solution and irradiated under N_2O with a dose of 20 Gy. As in the first described system, N_2O scavenged hydrated electrons, and α-hydroxyalkyl radicals were formed in the course of reactions 5−8. They reacted with thiol according to reaction 15 (see Table 1), forming thiyl radicals ($RS^\bullet$). Subsequently, thiyl radicals reacted with thiolate (reaction 16), which led to the formation of the broad absorption maximum of disulfide radical anion at 420 nm (Figure 3). Reactions 15 and 16, as well as their rate constants used in the modeling procedure, are given in the Table 1.

For cysteamine thiyl radicals at pH = 9.5, reaction 16 has a rate constant $k_{16} = 3.4 \times 10^9$ dm^3 mol^{-1} s^{-1}, while the dissociation takes place with $k_{-16} = 1.9 \times 10^6$ s^{-1}.[28] The equilibrium (16) is strongly pH dependent. Therefore, it was of crucial importance to adjust the pH value of the solution appropriately. It had to be kept higher than the pK_a of the sulfhydryl group of the thiol used. For cysteamine containing solutions, pH was fixed at 9.5−9.8 (pK_a (CystSH) = 8.3),[29] whereas, for 2-mercaptoethanol containing solutions, 10.5−10.8 pH was used (pK_a (MerSH) = 9.5).[29] It was adjusted by adding borate buffer (2.5×10^{-2} mol dm^{-3}). Thiols used in the experiments were aliphatic ones, so their thiyl radicals reacted with residual oxygen according to reaction 17.[30] Moreover, the observed monitoring species itself was oxygen sensitive (reac-

TABLE 1: Reactions 15 and 16 with the Rate Constants Used in the Modeling Procedure

		rate constant used in the modeling procedure			
		k_{15}, k_{16} [dm^3 mol^{-1} s^{-1}]		k_{-15} [dm^3 mol^{-1} s^{-1}] k_{-16} [s^{-1}]	
reaction	reaction number	CystSH	MerSH	CystSH	MerSH
^{i}Pr$^\bullet$OH + RSH ⇄ ^{i}PrOH + RS$^\bullet$	15	3.5×10^8	5.5×10^8	1.5×10^4	9.0×10^3
RS$^\bullet$ + RS$^-$ ⇄ RSSR$^{\bullet -}$	16	3.5×10^9	4.8×10^9	1.0×10^6	2.6×10^6

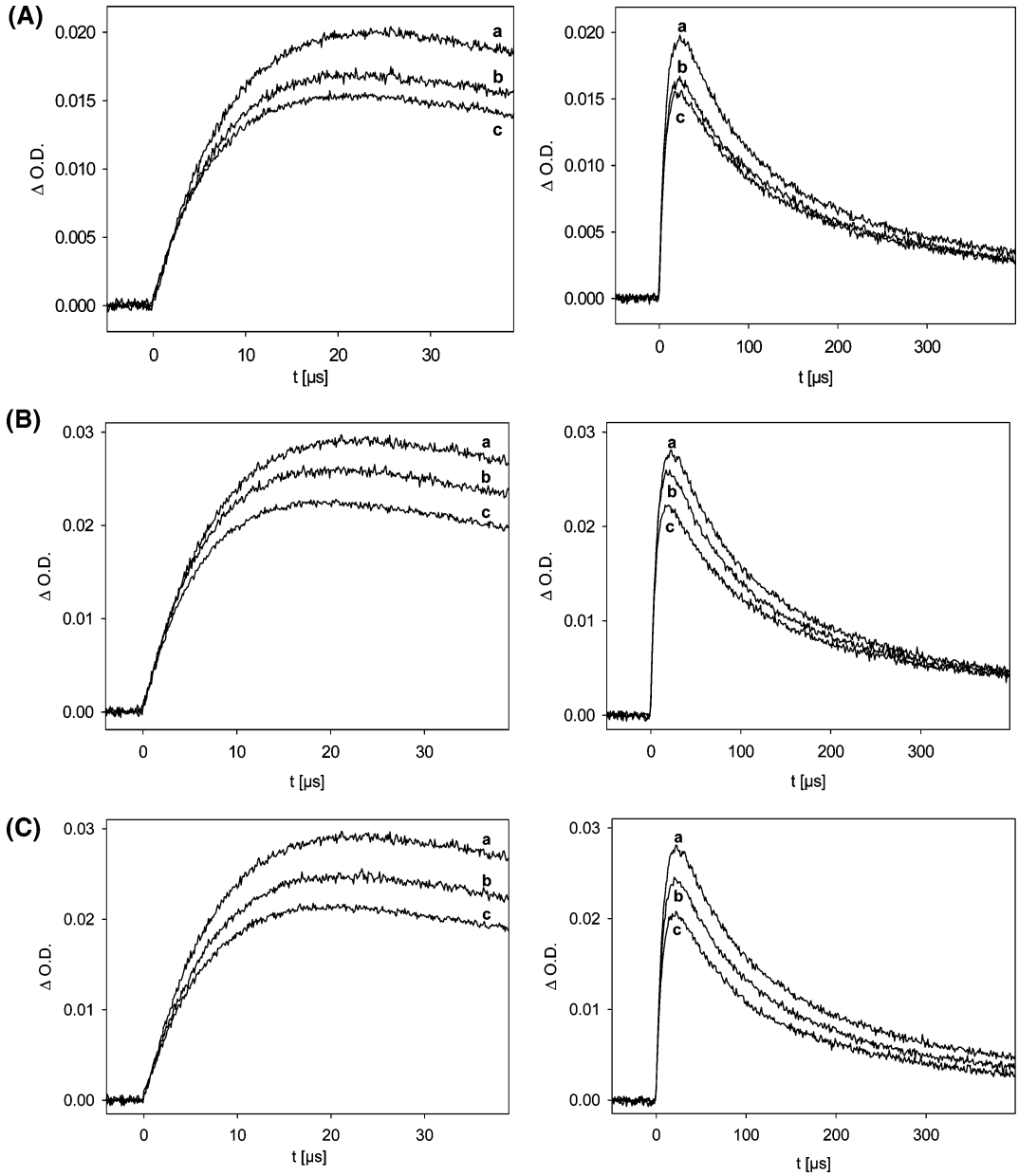

Figure 4. Time profiles at 420 nm for various (A) thymine, (B) uracil, and (C) cytosine concentrations; (a) 0, (b) 1×10^{-2}, and (c) 2×10^{-2} mol dm^{-3} concentration of pyrimidine in N_2O saturated water/2-propanol (17:3, v/v) solutions of cysteamine hydrochloride (2×10^{-3} mol dm^{-3}); pH = 9.5−9.9, adjusted with borate buffer; dose/pulse, 20 Gy.

tion 18).[31] Therefore, it was very important to ensure a constant amount of residual oxygen.

$$RS^{\bullet} + O_2 \rightleftarrows RSOO^{\bullet} \qquad k_{17} = 2.0 \times 10^9 \text{ dm}^3 \text{ mol}^{-1} \text{ s}^{-1}$$
$$k_{-17} = 6.0 \times 10^5 \text{s}^{-1} \quad (17)$$

$$RSSR^{\bullet -} + O_2 \rightleftarrows RSSR + O_2^{\bullet -}$$
$$k_{18} = 8.0 \times 10^8 \text{ dm}^3 \text{ mol}^{-1} \text{ s}^{-1} \quad (18)$$

The dose used was also influencing the decay of the observed species as the result of the recombination reaction of thiyl radicals (Schemes 1 and 2), occurring with the rate constant $2k = 3.5 \times 10^9$ dm^3 mol^{-1} s^{-1}.[32] First, measurements without pyrimidine took place, then the experiments in the presence of 1×10^{-2} and 2×10^{-2} mol dm^{-3} thymine, uracil, and cytosine were carried out. As expected from the competition between reactions 4 and 16 for all three pyrimidines, considerable lowering of the amplitude at 420 nm was observed; however, kinetics of the formation and decay remained practically unchanged (Figure 4). No additional absorption appeared in the measured region. Results presented in Figure 4 concern cysteamine hydrochloride. Analogous studies were performed for 2-mercaptoethanol (not shown here). All the experiments were carried out for cysteamine as well as for mercaptoethanol-containing solutions in the presence of various pyrimidines under concentration variation. Comparative experiments were made with samples containing 4×10^{-2} mol dm^{-3} *cis*-hexenol, which was used as an unsaturated model compound. Here, the lowering of the amplitude at 420 nm was also observed, again without any significant changes in kinetics. The decrease of the amplitude for 4×10^{-2} mol dm^{-3} *cis*-hexenol appears to be slightly smaller (≈15%), as in the case of samples containing 2×10^{-2} mol dm^{-3} pyrimidines (≈25%).

3.1.3. Monitoring Based on the Pentadienyl Radical Absorption. Thiyl radicals are capable of abstracting hydrogen from

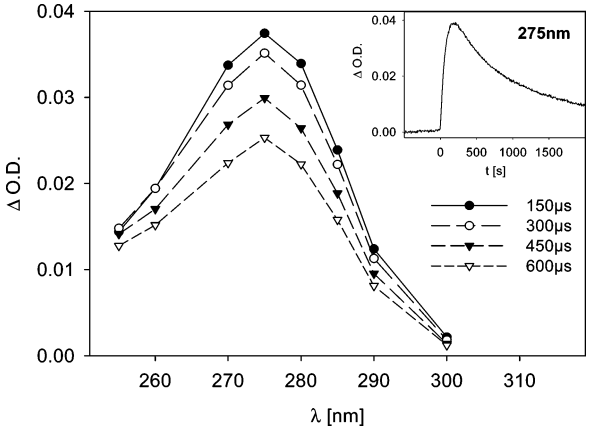

Figure 5. Decay in time of pentadienyl radical absorption; N_2 saturated water/ethanol (1:1, v/v) solution of linoleic acid (1×10^{-3} mol dm^{-3}), cysteamine hydrochloride (1.3×10^{-3} mol dm^{-3}), and 2-chloroethanol (0.1 mol dm^{-3}); dose/pulse, 10Gy. The inset shows time profile at 275 nm.

bisallylic methylene groups in PUFA. As the result of that abstraction reaction, pentadienyl radicals (LA$^{\bullet}$) exhibiting pronounced absorption at 275 nm are formed.[10,12,33] We expected that the addition of pyrimidines should influence the absorption of pentadienyl radicals because of the competition between pentadienyl radical formation (reaction 21; see Table 2) and the reaction of thiyl radicals with pyrimidine (reaction 4). To prove it, solutions of 1×10^{-3} mol dm^{-3} linoleic acid and 1.3×10^{-3} mol dm^{-3} cysteamine hydrochloride (or 1×10^{-3} mol dm^{-3} 2-mercaptoethanol) in a solvent mixture of ethanol/water (1:1, v/v) were irradiated under nitrogen with 10 and 20 Gy/pulse dose. For electron scavenging, 0.1 mol dm^{-3} 2-chloroethanol was used (reaction 19):

$$ClCH_2CH_2OH + e_{aq}^{-} \rightarrow {}^{\bullet}CH_2CH_2OH + Cl^{-} \qquad k_{19} = 4.2 \times 10^8 \text{ dm}^3 \text{ mol}^{-1} \text{ s}^{-1} \quad (19)$$

The absorption of pentadienyl radical could be observed with a sharp maximum at 275 nm (Figure 5). The α-hydroxyalkyl radicals were generated from ethanol in the reactions analogous to 5, 7, and 8. They were abstracting hydrogen from the thiol according to reaction 20 (see Table 2). Thiyl radicals, once generated, interacted with PUFA in two ways: reversibly adding to the double bonds[10,12,33] and abstracting hydrogen from bisallylic methylene group and forming pentadienyl radicals. Taking the first path (addition) as constant and invisible part, the second part (reaction 21) was used for monitoring the thiyl radicals. According to the literature data the abstraction reaction 21 occurs with the rate constants $k_{21} = 2.5-3.1 \times 10^7$ dm^3 mol^{-1} s^{-1}, whereas the back reaction is much slower: $k_{-21} \leq 1.0 \times 10^5$ dm^3 mol^{-1} s^{-1}.[10,12,33] Reactions 20 and 21 are given in the Table 2, with their rate constants used in the modeling procedure.

When the pyrimidines (thymine, uracil, cytosine) were added to the system (0.5×10^{-3}, 1×10^{-3}, 2×10^{-3}, and 5×10^{-3} mol dm^{-3}), a considerable lowering of the amplitude without any significant changes in kinetics was observed, see Figure 6. It was impossible to make observations at 275 nm because of the high ground-state absorption of the pyrimidines at this wavelength; therefore, as a detection wavelength, 290 nm was chosen. The generated aliphatic thiyl radicals are oxygen sensitive. Also the carbon-centered bisallylic radicals (LA$^{\bullet}$, i.e., the observed species) are oxygen sensitive (reaction 22); $k_{22} = 5.4 \times 10^8$ dm^3 mol^{-1} s^{-1}.[10] Comparative experiments with *cis*-

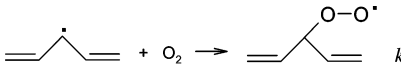

$$k_{22}=5.0\times10^8 \text{ dm}^3 \text{ mol}^{-1} \text{ s}^{-1} \quad (22)$$

hexenol (4×10^{-2} mol dm^{-3}) as an unsaturated model compound were also carried out. For *cis*-hexenol, the effect could be monitored at 275 nm. Again, lowering of the amplitude was observed without significant changes in the kinetics. As described already in the former paragraph, the interaction of thiyl radicals with *cis*-hexenol was less efficient than the one observed for the pyrimidines.

3.2. Kinetic Simulations of the Observed Time Profiles. Because of the very complex kinetics, a simple treatement of the data with Stern−Volmer plots was impossible. To obtain the rate constants of thiyl radical addition and elimination of the pyrimidine C5−C6 double bond (k_4 and k_{-4}), the experimentally obtained time profiles were simulated with a modified version of ACUCHEM (computer program for modeling complex reaction systems)[18], the Win95 Simac3.3. This program solves a set of differential equations. The number of equations is equal to the number of reactions included in the assumed reaction scheme. Two reaction schemes, for the monitoring systems described in Parts 3.1.2. and 3.1.3., were developed as a basis for the kinetic simulations (Schemes 1 and 2). Although they seem very complicated, the reaction mechanisms can be understood by considering the main reaction paths leading to the formation of the observed species: RSSR$^{\bullet-}$ and LA$^{\bullet}$, which were used to monitor reaction 4. All the other reactions are either recombination reactions or reactions with residual oxygen, which are typical for carbon-centered radicals. Possibly also, repair reactions take place (reactions 26 and 27), which are, however, of minor importance. The majority of the reactions included in the schemes were already known before; therefore, all of them were given certain rate constants on the basis of the existing literature data and our own measurements. k_4 and k_{-4} were a matter of the fit operations, i.e., they were adjusted during simulation procedure to obtain the best correlation between the experimental and simulated time profile (Figure 7). The obtained rate constants are given in Table 3. For the addition of thiyl radicals to the pyrimidine C5−C6 double bond, values of the rate constants are in the 10^7 dm^3 mol^{-1} s^{-1} magnitude order; the elimination rate constants are in the 10^5 s^{-1} magnitude order.

3.3. Quantum Chemical Calculations. Quantum chemical calculations were made at the B3LYP/6-31G(d)/PCM level. The C5−S and C6−S bonds lengths in the Pyr$^{\bullet}$(RS) were determined as well as the enthalpies of the addition reaction, depending on the regiochemistry (addition to the C5 or to the C6 position) and HOMO and LUMO energies. Calculations were made also for cyclohexane and *cis*-hexenol. Because they have a double bond as a potential site of thiyl radical addition, they can serve

TABLE 2: Reactions 20 and 21 with the Rate Constants Used in the Modeling Procedure

		rate constant used in the modeling procedure			
		k [dm^3 mol^{-1} s^{-1}]		k_- [dm^3 mol^{-1} s^{-1}]	
reaction	reaction number	CystSH	MerSH	CystSH	MerSH
$CH_3CH^{\bullet}OH + RSH \rightleftarrows EtOH + RS^{\bullet}$	20	9.0×10^7	1.3×10^8	1.3×10^4	5.0×10^3
$RS^{\bullet} + LA \rightleftarrows RSH + LA^{\bullet}$	21	8.0×10^6	1.5×10^7	5.0×10^4	5.0×10^4

SCHEME 1: Reaction Scheme for the Monitoring System Based on the Disulfide Radical Anion Absorption

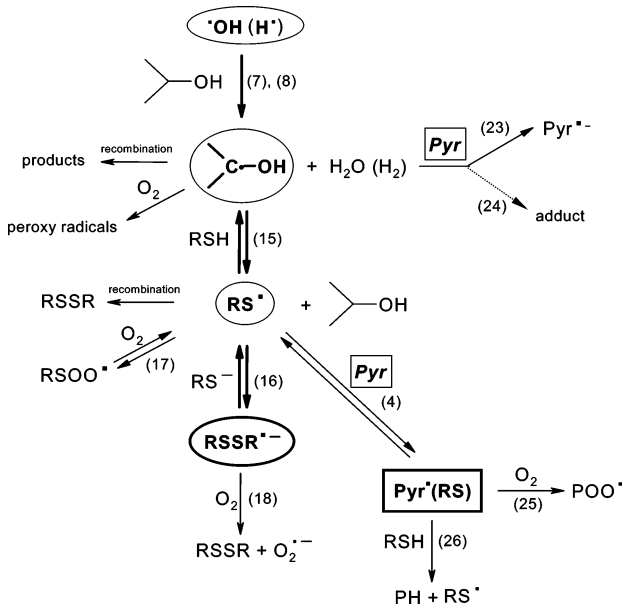

Species given in the circles are formed in the main reaction pathway leading to the $RSSR^{\bullet-}$ formation (framed with bold-line circle) observed at 420 nm. Addition of pyrimidines (squares) leads to the reactions 4, 23, and 24. Product of the reaction 4 is given in a bold-line square frame. Dotted-line arrow is used for reaction 24, indicating that this reaction can be neglected because of the small rate constant. Hydrated electrons are not marked on the given scheme because they are scavenged in the reaction with N_2O (reaction in the text) leading to $HO^{\bullet}$ radicals formation.

SCHEME 2: Reaction Scheme for the Monitoring System Based on the Pentadienyl Radical Absorption

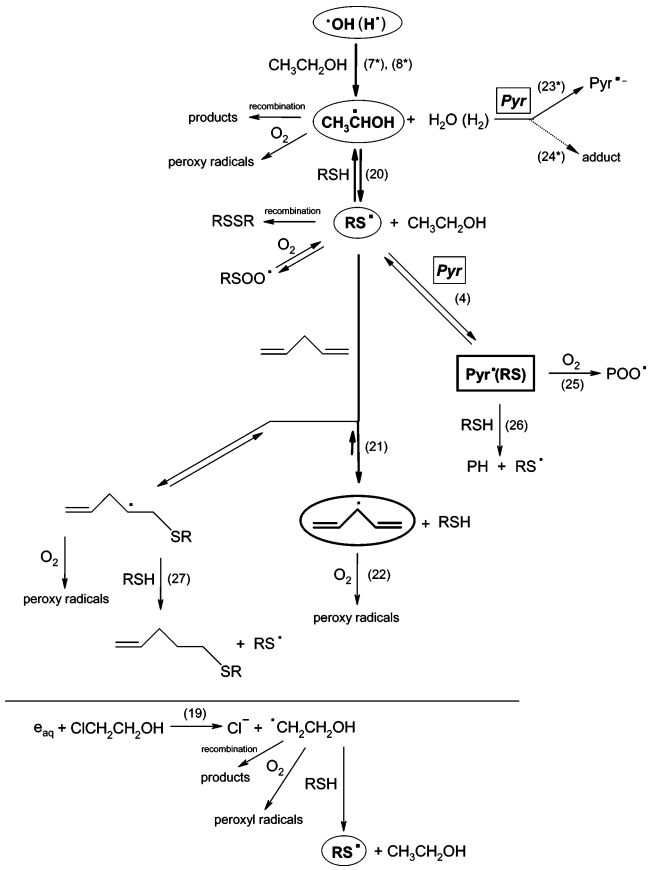

Species given in the circles are formed in the main reaction pathway leading to the $LA^{\bullet}$ formation (framed with bold-line circle) observed at 290 nm. Addition of pyrimidines (squares) leads to the reactions 4, 23*, and 24*. Product of reaction 4 is given in a bold-line square frame. Dotted-line arrow is used for reaction 24*, indicating that this reaction can be neglected because of the small rate constant. Hydrated electrons are marked on the scheme, because as the result of their scavenging in reaction 19 β-hydroxyalkyl radicals are formed, which further react with the thiol giving thiyl radicals.

as reference compounds. The obtained values are given in Table 4. The calculated C−S bond length in the thiyl radical is 1.816 Å, the C−S bond length in the thiyl radical when bound to pyrimidine is 1.840 Å, and the SOMO energy of the thiyl radical is −89.94 kcal mol^{-1}.

4. Discussion

4.1. Results of Pulse Radiolysis Experiments and Their Evaluation by Kinetic Simulations. Results presented for the aromatic thiols indicate that aromatic thiyl radicals react with the pyrimidine C5−C6 double bond with $k_{10} \leq 1 \times 10^4$ dm^3 mol^{-1} s^{-1}, which is out of our experimental observation range. Low reactivity of aromatic thiyl radicals is probably connected with their resonance stabilization. For the aliphatic thiyl radicals, however, that kind of interaction was undoubtedly seen by monitoring methods based on the competition kinetics (Figures 4 and 6). The direct detection with the use of aliphatic thiyl radicals was not successful (Figure 2). These experiments, however, gave data which were helpful in the interpretation of the results obtained by $RSSR^{\bullet-}$ and $LA^{\bullet}$ monitoring systems.

Direct detection was impossible because of the electron-transfer reaction from α-hydroxyalkyl radicals to pyrimidines, leading to pyrimidine radical anion ($Pyr^{\bullet-}$) formation (reaction 23 on Scheme 1 and 23* on Scheme 2). Pyrimidine radical anions and their oxygen-protonated forms absorb in the region 270−350 nm and have extinction coefficients around 1000−1500 M^{-1} cm^{-1}.[34,35,36] Their presence could explain the lack of distinct changes at 330 nm for all three pyrimidines. C6−Protonated radical anions of thymine and uracil absorb in the region 380−430 nm with the extinction coefficients around 1100 M^{-1} cm^{-1}, which corresponds to the new absorption band observed for those pyrimidines.[37] Such absorption could be easily registered because, apart from weak absorption of penicillamine thiyl radicals and isopropyl radicals, there were no other species exhibiting strong absorption in the investigated wavelength range.

We have no clear explanation of the new absorption band appearing at 480 nm in the presence of cytosine. So far, there is no evidence of cytosine radical anion protonation at C5 or C6 in aqueous solution. There is only information on hydrogen atom addition to C5 and C6 position in a solid state.[38] The spectrum of the adduct of the hydrogen radical to the C6 position of the cytosine ring was calculated ab initio.[39] It should exhibit absorption maximum in the range around 430−460 nm.[39] Under our experimental conditions, cytosine exists in the protonated form ($pK_a = 4.45$).[40] Hence, if the electron transfer from isopropyl radical occurs, its product should be a neutral species. That is different from the situation that takes place in the case of thymine and uracil, where at first a radical anion is formed, then it undergoes protonation. We cannot exclude that the species absorbing at 480 nm is analogous to the C5- or C6-protonated radical anions of uracil or thymine.

Apart from the absorption at 400, 420, and 480 nm, we did not observe any other changes in the measured region; therefore, we concluded that the adduct $Pyr^{\bullet}(RS)$ either does not absorb in that range or its absorption is too small to be detected.

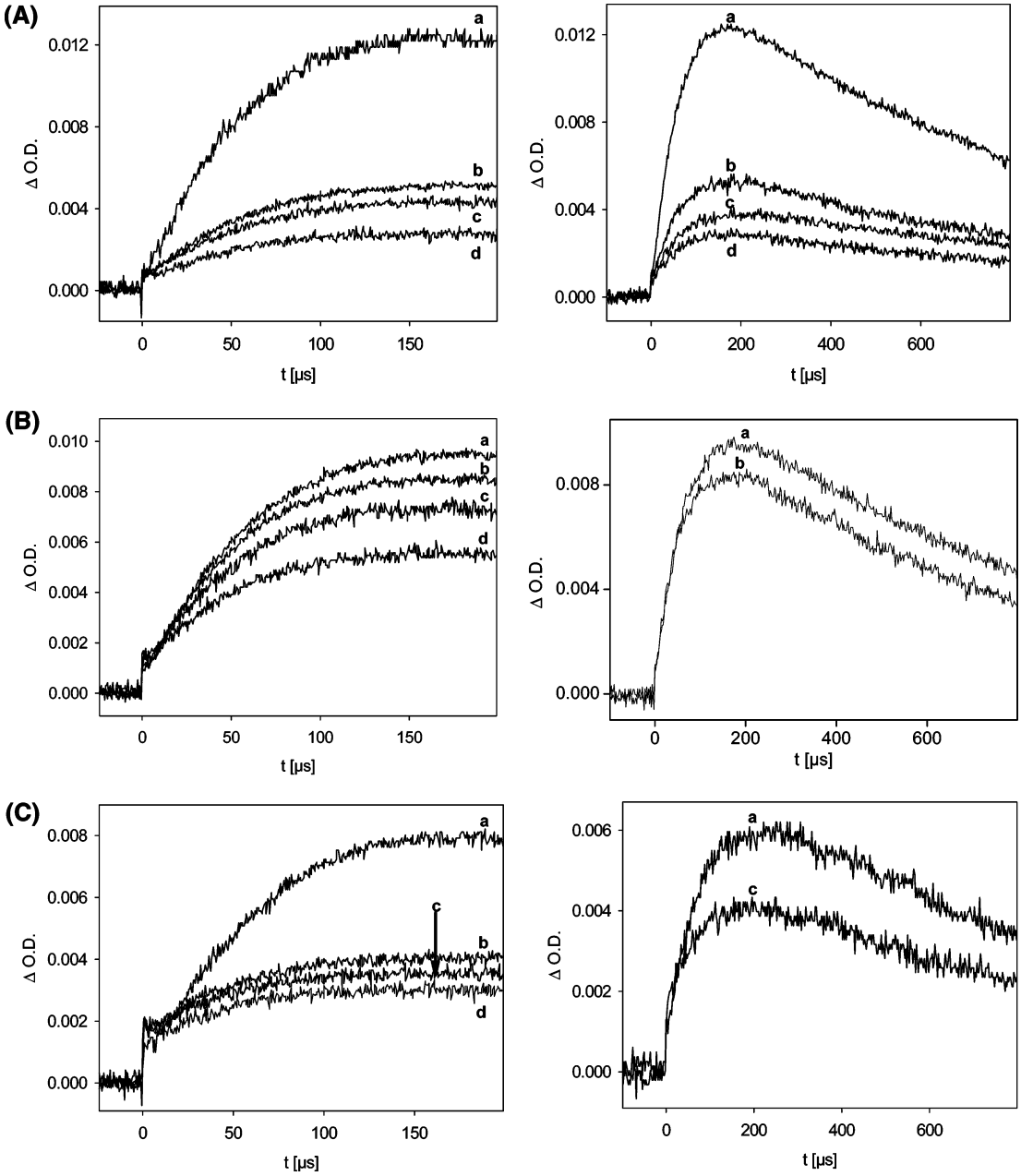

Figure 6. Time profiles at 290 nm for various (A) thymine (a) 0, (b) 0.5×10^{-3}, (c) 1×10^{-3}, and (d) 2×10^{-3} mol dm^{-3}; (B) uracil (a) 0, (b) 1×10^{-3}, (c) 2×10^{-3}, and (d) 5×10^{-3} mol dm^{-3}; (C) cytosine (a) 0, (b) 0.5×10^{-3}, (c) 1×10^{-3}, and (d) 2×10^{-3} mol dm^{-3} concentrations in N_2-saturated water/ethanol (1:1, v/v) solutions of linoleic acid (1×10^{-3} mol dm^{-3}), cysteamine hydrochloride (1.3×10^{-3} mol dm^{-3}), and 2-chloroethanol (0.1 mol dm^{-3}); dose/pulse, 10 Gy.

4.1.1. RSSR$^{\bullet-}$ Monitoring System. The addition of the tested pyrimidines caused significant lowering of the amplitude of the observed species, practically without influencing the shape of the time profiles. It can be explained only in terms of thiyl radical interaction with the C5−C6 double bond in pyrimidines: part of the thiyl radicals as the result of reaction 4 is "blocked" in the form of the adduct Pyr$^{\bullet}$(RS), therefore, less thiyl radicals can take part in the reaction, leading to the formation of the observed species. Because reaction 4 is reversible and the back reaction occurs with a pretty high rate constant (Table 3), changes in the kinetics are only of minor importance. There are two reactions that can possibly shift the equilibrium of reaction 4 in the direction of the adduct formation. These are the reaction of the Pyr$^{\bullet}$(RS) with residual oxygen (reaction 25 on Scheme 1) and the repair reaction in which thiyl radicals are regenerated (reaction 26 on Scheme 1).

To describe the complex system in detail, we have to consider that added pyrimidines react not only with thiyl radicals, but also with α-hydroxyalkyl radicals according to the reactions 23 and 24 in Scheme 1. The electron-transfer reaction 23 should be taken into account because reaction 15 will be only ∼20 times faster; for example, for thymine, $[T]_{max} = 2 \times 10^{-2}$ mol dm^{-3}, $k_{23} = 1 \times 10^6$ dm^3 mol^{-1} s^{-1} and [CystSH] $= 2 \times 10^{-3}$ mol dm^{-3}, $k_{15} = 2.0 \times 10^8$ dm^3 mol^{-1} s^{-1}.[41,42] As the result of reaction 23, part of the α-hydroxyalkyl radicals react with the pyrimidine. Moreover, in solutions containing 2×10^{-2} mol dm^{-3} pyrimidine, hydrated electrons are not completely scavenged by N_2O, and part of them add to the pyrimidine molecule, forming a pyrimidine radical anion (reaction 28) analogous to the one formed in reaction 23 (Scheme 1).

$$e_{aq}^- + \text{Pyr} \rightarrow \text{Pyr}^{\bullet-} \qquad (28)$$

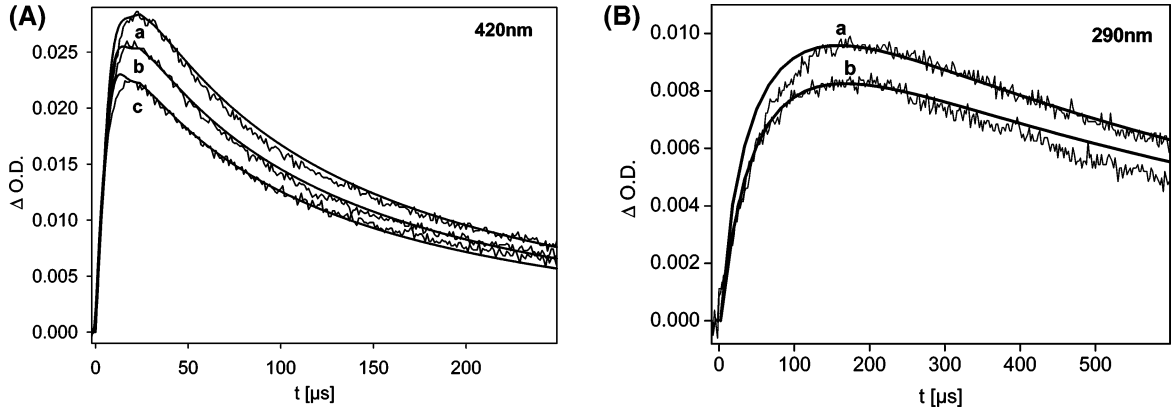

Figure 7. Experimental and simulated time profiles for two different detection systems. (A) Decays at 420 nm with various uracil concentrations (a) 0, (b) 1×10^{-2}, and (c) 2×10^{-2} mol dm^{-3} in N_2O saturated water/2-propanol (17:3, v/v) solution of 2×10^{-3} mol dm^{-3} cysteamine hydrochloride; pH = 9.5−9.9, adjusted with borate buffer; dose/pulse, 20 Gy. (B) decays at 290 nm with various uracil concentrations (a) 0 and (b) 1×10^{-3} mol dm^{-3} in N_2-saturated water/ethanol (1:1, v/v) solutions of 1×10^{-3} mol dm^{-3} linoleic acid, 1.3×10^{-3} mol dm^{-3} cysteamine hydrochloride, and 0.1 mol dm^{-3} 2-chloroethanol; dose/pulse, 10 Gy.

TABLE 3: Summary of the Rate Constants Obtained by Kinetic Simulations[a]

	monitoring by RSSR$^{\bullet-}$ absorption				monitoring by LA$^{\bullet}$ absorption			
	addition Pyr + RS$^{\bullet}$ $k_4 \times 10^{-7}$ dm^3 mol^{-1} s^{-1}		elimination $k_{-4} \times 10^{-5}$ s^{-1}		addition Pyr + RS$^{\bullet}$ $k_4 \times 10^{-7}$ dm^3 mol^{-1} s^{-1}		elimination $k_{-4} \times 10^{-5}$ s^{-1}	
	CystSH	MerSH	CystSH	MerSH	CystSH	MerSH	CystSH	MerSH
thymine	1.0	1.2	1.5	1.6	3.0	1.0	1.0	1.0
uracil	1.0	1.2	1.5	2.0	1.0	3.0	1.0	0.7
cytosine	2.5	1.8	1.5	1.2	3.0	1.0	0.9	1.0
cis-hexenol	0.1[b]	0.4	0.1[b]	1.2	0.1	0.1	2.0	2.0

[a] For the RSSR$^{\bullet-}$ monitoring system, error of the given values is within ±25%, and for the LA$^{\bullet}$ monitoring system within ±35%. [b] Such small rate constants may be due to the experimental limitations.

TABLE 4: Parameters Obtained from Quantum Chemical Calculations at the B3LYP/6-31G(d)/PCM Level

unsaturated compound	bond length C5−S [Å]	bond length C6−S [Å]	$\Delta H(5)$ [kcal mol^{-1}]	$\Delta H(6)$ [kcal mol^{-1}]	HOMO energy [kcal mol^{-1}]	LUMO energy [kcal mol^{-1}]
cis-hexenol	1.903	1.910	−3.4	−3.3	−148.74	19.14
cyclohexene	1.856	1.856	−1.8	−1.8	−146.44	21.22
thymine	1.965	1.913	+6.4	+1.8	−147.36	−20.06
uracil	1.941	1.922	+3.7	+4.4	−151.97	−21.22
cytosine	1.967	1.940	+4.2	+3.7	−143.67	−15.68

As the result of both described reactions, at the first glance, fewer thiyl radicals should be formed, which should decrease the amplitude at 420 nm. However, under experimental conditions, the pyrimidine radical anion undergoes protonation at carbon 5 or 6[37] (reaction 29), and in this form is "repaired" by the added thiol (reaction 30), which regenerates thiyl radicals.

$$\mathrm{Pyr}^{\bullet-} \xrightarrow{\mathrm{H_2O(H+)}} \mathrm{Pyr}^{\bullet}\mathrm{(C6H)} \qquad (29)$$

$$\mathrm{Pyr}^{\bullet}\mathrm{(C6H)} + \mathrm{RSH} \rightarrow \mathrm{PyrH_2} + \mathrm{RS}^{\bullet} \qquad (30)$$

According to the results of the kinetic simulations discussed subsequently, the experimentally observed decrease is dominated by reaction 4, i.e., thiyl radical addition to the pyrimidine C5−C6 double bond. The addition of α-hydroxyalkyl radicals to the pyrimidine C5−C6 double bond (reaction 24 on Scheme 1) can be neglected because of the very low rate constant $k_{24} \leq 10^4$ dm^3 mol^{-1} s^{-1}.[43] All reactions discussed in this paragraph can be formally summarized in the way of a simple thiyl radical formation, i.e., all reaction paths generate these species. Therefore, in our simulation operations, we used only the simplified version of the thiyl radicals formation via the $^{\bullet}$OH reaction (reactions 5, 6, 8, and 15).

4.1.2. LA$^{\bullet}$ Monitoring System. The experimentally observed lowering of the amplitude in the presence of pyrimidines can be explained in terms of reaction 4, analogously as it was described in paragraph 4.1.1. for the RSSR$^{\bullet-}$ monitoring system. For the LA$^{\bullet}$ monitoring system, however, we can neglect the electron transfer reaction between α-hydroxyalkyl radicals and pyrimidines (reaction 23* in Scheme 2). Under the given experimental conditions, ethanol-derived α-hydroxyalkyl radicals react with the thiol (reaction 20) ∼100 times faster than with the added pyrimidine (for example for thymine: $[T]_{max} = 2 \times 10^{-3}$ mol dm^{-3}, $k_{23*} = 1 \times 10^6$ dm^3 mol^{-1} s^{-1}, and [CystSH] = 1.3×10^{-3} mol dm^{-3}, $k_{20} = 1.7 \times 10^8$ dm^3 mol^{-1} s^{-1}).[41,42] Only for a few experiments in which 5×10^{-3} mol dm^{-3} pyrimidine was used, it is advantageous to consider reaction 23*, because reaction 20 will be only ∼45 times faster. As in the disulfide radical anion system, the addition of α-hydroxyalkyl radicals to the pyrimidine C5−C6 double bond (reaction 24* in Scheme 2) can be neglected.

4.1.3. Kinetic Simulations and Error Estimation. Because of our systems' complexity, it was impossible to estimate k_4 and k_{-4} in any other way than by kinetic simulations mentioned in the Results Section. We did not obtain a perfect fit, but with a set of rate constants, we were able to simulate the kinetic behavior of the investigated monitoring systems under all experimental conditions. Rate constants for the recombination reactions, reactions with residual oxygen, and other side

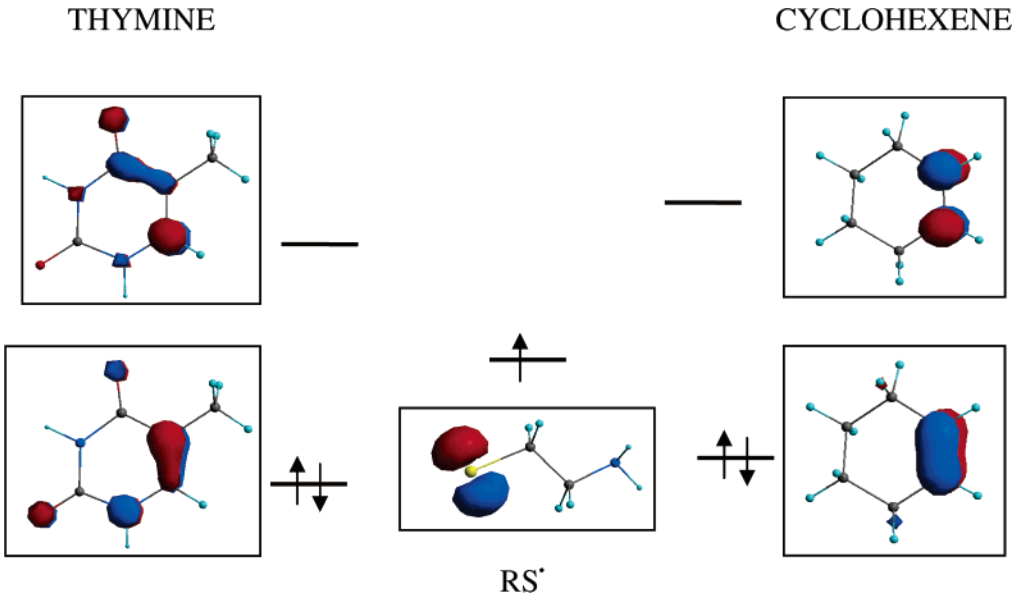

Figure 8. Energy levels of the molecular orbitals and the electron-density distribution in thymine and cyclohexene molecules as well as in thiyl radical calculated at the B3LYP/6-31G(d)/PCM level.

reactions were taken from the literature and treated in most of the cases as fixed values. The rate constants for the main reaction path, leading to the formation of the observed species, were in the simulation procedure because of their strong influence on the simulated time profiles, slightly changed in comparison to the literature values in order to obtain the best correlation between fitted curves and the experimental ones. This change in most of the cases was not higher than ±20%, i.e., the error given for most of the rate constants in the literature. The correlation between the simulated curves and the experimental ones was checked for thiols in different concentrations in the absence of pyrimidines to confirm that the created reaction schemes and used rate constants really reflect behavior of the investigated systems. The rate constants obtained in the described manner were reliable enough to be used for k_4 and k_{-4} determination.

Kinetic simulations were also carried out for *cis*-hexenol, which was used in the experiments as a model compound. Estimated rate constants for thiyl radicals addition to the *cis*-hexenol double bond are smaller than the corresponding values for pyrimidines (Table 3). This observation is in agreement with the experimental results, which show that, in both monitoring systems, changes induced by *cis*-hexenol addition were smaller in comparison to the changes caused by pyrimidines. This difference can be possibly explained in terms of the dynamics of both systems; while pyrimidine-like structures are rigid ones, the *cis*-hexenol molecule is very flexible.

It should be stressed that the values of the addition (k_4) and elimination (k_{-4}) rate constants determined on the basis of the experimental data from two completely different monitoring systems are consistent. Because kinetic simulations were carried out for both systems for a complete set of experimental data, the error of the given rate constants (Table 3) does not exceed ±25% (values obtained from the $RSSR^{\bullet-}$ monitoring system) and ±35% (values obtained from the $LA^{\bullet}$ monitoring system).

4.2. Quantum Chemical Calculations. There are two possibilities of thiyl radical interaction with the C5−C6 double bond in pyrimidines. The charge density can be shifted from pyrimidine HOMO to thiyl radical SOMO or from thiyl radical SOMO to pyrimidine LUMO. Energy levels of the molecular orbitals, together with the electron density distribution within chosen molecules, are given in Figure 8. Interaction between the pyrimidine C5−C6 double bond and the thiyl radical is weak because of two reasons; one is the big energy difference between pyrimidine HOMO and thiyl radical SOMO: 57.42, 62.03, 53.73 kcal mol^{-1} for thymine, uracil, and cytosine, respectively. The second is the weak Coulombic interaction between the pyrimidine molecule and the thiyl radical. That is reflected also in the enthalpy values (ΔH) of reaction 4 given in Table 4. For all pyrimidines, ΔH has a slightly positive value; for thiyl radical addition to the C6 position in the pyrimidine ring ($\Delta H(6)$) those values seem to be slightly lower. The fact that all of them are close to zero suggests that one can also expect an elimination reaction.[43,44] Bigger differences concerned with the addition of the thiyl radical either to the C5 or to the C6 position of the pyrimidine ring are visible when C5−S and C6−S bond lengths are considered; C6−S bond lengths are for all pyrimidines smaller than those of C5−S, which indicates that C6−S bonds are stronger. Therefore addition at the C6 position seem to be more probable.

Calculations were also made for two other molecules, for cyclohexene and *cis*-hexenol. Values of ΔH obtained for those molecules are all slightly negative, together with the much shortened C−S bond lengths in adduct molecules in comparison with C−S bond lengths in adducts of pyrimidines. This would indicate slightly bigger reactivity of thiyl radicals toward those molecules than toward pyrimidines. Because HOMO energies of pyrimidines, cyclohexene, and *cis*-hexenol are comparable, the difference must be connected with electron density distribution within unsaturated molecules. In the case of pyrimidines, it is spread all over the molecule, while in cyclohexene and *cis*-hexenol, it is concentrated in the region of double bond. Those considerations take into account only the thermodynamic aspect of the thiyl radicals interaction with unsaturated bonds. However, the experiments show that one has to consider also the fact that pyrimidine molecules are planar, while molecules of *cis*-hexenol as well as cyclohexene are not. Reaction can be to some extent kinetically controlled. The reactivity of the pyrimidines and *cis*-hexenol observed in the experiments is opposite to that arising from the quantum chemical calculations.

Conclusions

Thiyl radicals interact with the pyrimidine C5−C6 double bond by adding reversibly to the C6 position in the ring. Addition occurs with $k_4 = 1.0-3.0 \times 10^7$ dm^3 mol^{-1} s^{-1} and elimination with $k_{-4} = 0.7-2.0 \times 10^5$ s^{-1}, as determined from kinetic simulations. That kind of interaction is rather weak, which was confirmed by quantum chemical calculations, and probably does not depend strongly on the pyrimidine and thiol used. The adduct either does not absorb in the measured region or its absorption is too weak to be detected. Pyrimidines are building elements of nucleic acids, and any change in their structure can appear to be very important. Therefore, it is possible that interaction between thiyl radicals and the C5−C6 double bond in pyrimidines described in this paper, if it takes place also in living systems, is not without biological consequence.

Acknowledgment. The financial support from European Research Training Network SULFRAD (contract number HPRN-CT-2002-00184) is gratefully acknowledged. We thank Mr L. Richter for his help with pulse radiolysis equipment.

References and Notes

(1) Akhlaq, M. S.; Schuchmann, H.−P.; v. Sonntag, C. *Int. J. Radiat. Biol.* **1987**, *51*, (1), 91−102.

(2) Becker, D.; Summerfield, S.; Gillich, S.; Sevilla, M. D. *Int. J. Radiat. Biol.* **1994**, *65*, (5), 537−548.

(3) Milligan, J. R.; Tran, N. Q.; Ly, A.; Ward, J. F. *Biochemistry* **2004**, *43*, 5102−5108.

(4) *Oxidative Stress: Oxidants and Antioxidants*; Sies, H., Ed.; Academic Press: London, 1991.

(5) von Sonntag, C. *The Chemical Basis of Radiation Biology*; Taylor & Francis: London, 1987.

(6) Schöneich, C.; Asmus, K. D.; Bonifačić, M. *J. Chem. Soc., Faraday Trans.* **1995**, *91*, (13), 1923−1930.

(7) Nauser, T.; Schöneich, C. *Chem. Res. Toxicol*. **2003**, *16*, 1056−1061.

(8) Zhao, R.; Lind, J.; Merényi, G.; Eriksen, T. E. *J. Am. Chem. Soc*. **1994**, *116*, 12010−12015.

(9) Nauser, T.; Schöneich, C. *J. Am. Chem. Soc*. **2003**, *125*, 2042−2043.

(10) Schöneich, C.; Dillinger, U.; von Bruchhausen, F.; Asmus, K. D. *Arch. Biochem. Biophys.* **1992**, *292*, (2), 456−467.

(11) Chatgilialoglu, C.; Ferreri, C.; Ballestri, M.; Mulazzani, Q. G.; Landi, L. *J. Am. Chem. Soc*. **2000**, *122*, 4593−4601.

(12) Sprinz, H.; Schwinn, J.; Naumov, S.; Brede, O. *Biochim. Biophys. Acta* **2000**, *1483*, 91−100.

(13) Ferreri, C.; Samadi, A.; Sassatelli, F.; Landi, L.; Chatgilialoglu, C. *J. Am. Chem. Soc*. **2004**, *126*, 1063−1072.

(14) Chatgilialoglu, C.; Altieri, A.; Fischer, H. *J. Am. Chem. Soc*. **2002**, *124*, 12816−12823.

(15) Sprinz, H.; Adhikari, S.; Brede, O. *Adv. Colloid Interface Sci.* **2001**, *89*−*90*, 313−325.

(16) Kratzsch, S.; Drössler, K.; Sprinz, H.; Brede, O. *Arch. Biochemi. Biophys.* **2003**, *416*, 238−248.

(17) Carter, K. N.; Taverner, T.; Schiesser, C. H.; Greenberg, M. M. *J. Org. Chem*. **2000**, *65*, 8375−8378.

(18) Braun, W. at al. *Int. J. Chem. Kinet.* **1988**, *20*, 51−62.

(19) Brede, O.; Orthner, H.; Zubarev, V. E.; Hermann, R. *J. Phys. Chem.* **1996**, *100*, 7097−7105.

(20) Riyad, Y. M.; Hermann, R.; Brede, O. *Chem. Phys. Lett.* **2003**, *376*, 776−780.

(21) Ito, O.; Matsuda, M. *J. Am. Chem. Soc*. **1979**, *101*, 1815−1819.

(22) Ito, O.; Matsuda, M. *J. Am. Chem. Soc*. **1981**, *103*, 5871−5874.

(23) Ito, O.; Matsuda, M. *J. Am. Chem. Soc*. **1982**, *104*, 1701−1703.

(24) Purdie, J. W.; Gillis, H. A.; Klassen, N. V. *Chem. Commun.* **1971**, 1163−1165.

(25) Hoffman, M. Z.; Hayon, E. *J. Phys. Chem.* **1973**, *77*, 990−996.

(26) Buxton, G. V.; Greenstock, C. L.; Helman, W. P.; Ross, A. B. *J. Phys. Chem. Ref. Data* **1988**, *17*, 513−886.

(27) Hayon, E.; Hoffman, M. Z. *J. Am. Chem. Soc.* **1972**, *94*, 7950−7957.

(28) Mezyk, S. P. *J. Phys. Chem.* **1996**, *100*, 8295−8301.

(29) Fasman, G. D. *Handbook of Biochemistry and Molecular Biology, Physical and Chemical Data*, CRC Press Inc.: Boston, 1976.

(30) Zhang, X.; Zhang, N.; Schuchmann, H. P.; von Sonntag, C. *J. Phys. Chem*. **1994**, *98*, 6541−6547.

(31) Mićić, O. I.; Nenadović, M. T.; Carapellucci, P. A. *J. Am. Chem. Soc.* **1978**, *100*, 2209−2212.

(32) Hoffman, M. Z.; Hayon, E. *J. Phys. Chem.* **1973**, *77*, 990−996.

(33) Brede, O.; Schwinn, J.; Leistner, S.; Naumov, S.; Sprinz, H. *J. Phys. Chem. A* **2001**, *105*, 119−127.

(34) Hayon, E. *J. Chem. Phys.* **1969**, *51*, 4881−4892.

(35) Theard, L. M.; Peterson, F. C.; Myers, L. S. *J. Phys. Chem.* **1971**, *75*, 3815−3821.

(36) Hissung, A.; von Sonntag, C. *Int. J. Radiat. Biol.* **1979**, *35*, 449−458.

(37) Deeble, D. J.; Das, S.; von Sonntag, C. *J. Phys. Chem.* **1985**, *89*, 5784−5788.

(38) Flossmann, W.; Westhof, E.; Müller, A. *Int. J. Radiat. Biol.* **1976**, *30*, 301−315.

(39) Krauss, M.; Osman, R. *J. Phys. Chem. A* **1997**, *101*, 4117−4120.

(40) *CRC Handbook of Chemistry and Physics*; Lide, D. R., Ed.; CRC Press Inc.: Boca Raton, FL, 1992−93.

(41) Unpublished results; values of k_{21} slightly higher than values reported earlier by Steenken, S.; Telo, J. P.; Novais, H. M.; Candeias, L. P. *J. Am. Chem. Soc.* **1992**, *114*, 4701−4709.

(42) Nucifora, G.; Smaller, B.; Avery, E. C.; Remko, R. *Radiat. Res.* **1972**, *49*, 96−111.

(43) Schuchmann, H. P.; Wagner, R.; von Sonntag, C. *Int. J. Radiat. Biol.* **1986**, *50*, 1051−1068.

(44) Naumov, S.; von Sonntag, C. *J. Phys. Org. Chem*. in press.